20th International Conference on Structural Mechanics in Reactor Technology (SMiRT 20)
Espoo, Finland, August 9-14, 2009
SMiRT 20-Division 5, Paper 1840

Heat-mechanics Interaction Behavior of Lead Rubber Bearings for Seismic Base Isolation under Large and Cyclic Lateral Deformation Part 2: Seismic Response Analysis of Base Isolated Reactor Building Subjected to Horizontal Bi-Directional Earthquake Motions

Nobuhisa Sato[a], Shigeru Furukawa[b], Michiya Kuno[b], Ryu Shimamoto[b], Yasuo Takenaka[a], Takashi Nakayama[a] and Akihiro Kondo[a]

[a]Kajima Corporation, Tokyo, Japan, e-mail: satohno@kajima.com
[b]Chubu Electric Power Co. Inc,, Nagoya, Japan

Keywords: Base-isolated reactor building, Bi-directional earthquake motions, LRB, Fluctuation factors, Seismic response analysis, Lead temperature rise.

1 ABSTRACT

When applying a base isolation system to a reactor building located in a district of high seismic intensity, it is indispensable to understand fluctuations of seismic response caused by the changes of restoring force characteristics of the isolation device. Where lead rubber bearings are used for the isolation system, the temperature rise of the lead plug caused by absorption of the seismic energy decreases its yield stress, and this is one of the factors inducing response fluctuation. The orthogonal component of a horizontal earthquake motion is another factor influencing displacement response compared with the response under uni-directional earthquake motion. Environmental temperature, degradingness caused by passage of time and slight differences in the characteristics of individual isolation devices also have effects on seismic response. We conducted analytical studies to examine the degree of response fluctuation induced by each of these factors and combinations of factors using an assumed base-isolated reactor building model and several kinds of input earthquake motions. As a result, in this study, even when taking into account all fluctuation factors at the same time, increase in maximum displacement response stayed within 1.5 times as large as not taking into account the fluctuation factors.

2 INTRODUCTION

According to the Regulatory Guide for Aseismic Design of Nuclear Reactor Facilities in Power Plants, reactor buildings constructed in Japan before 2006 were required to be built on bedrock as rigid structures. However, the Regulatory Guide was revised in 2006, and allowed reactor buildings to use base isolation systems. Thus, increasing application of base-isolated structures to reactor buildings is expected because of their enhanced seismic safety.

Base-isolated structures are expected to be more suitable than rigid structures, especially in districts of high seismic intensity. In this study, Lead Rubber Bearings (LRB) were selected as isolation devices suitable for reactor buildings following parametrical analytical studies using many types of isolation devices. LRB has characteristic fluctuations caused by environmental temperature of the bearing, product deviation and aging. The yield stress of lead has thermal dependency, as discussed in Part 1. The restoring force characteristics of the LRB are altered by temperature rise of lead due to cyclic loading during a long-period strong earthquake. These characteristic fluctuations and alteration of restoring force characteristics of the LRB caused by temperature rise of lead affect the seismic response of a base-isolated building. The LRB has no directional dependency. Its behavior when subjected to bi-directional earthquake motions is different from that when subjected to uni-directional earthquake motion. However, the influences of these fluctuation factors and combinations on building response have not been studied for isolated reactor buildings located in districts of high seismic intensity. Therefore, we conducted an analytical study using an assumed base-

isolated reactor building located in a district of high seismic intensity to examine the influence of these fluctuations and combinations on building responses.

3 ANALYTICAL MODEL

3.1 Base isolation system

An LRB with a lead plug having twice the cross-sectional area of a standard type is assumed to be used in the base isolation system in this study. Therefore, it has higher damping characteristics than the standard one. Its specification is shown in table 1. Its natural vibration period based on rubber stiffness only is 3.93 seconds and its ratio of yield shear force to dead load is 0.139.

Table 1. Specifications of the LRB

Base isolation system	Elastic shear modulus of rubber (N/mm^2)	Diameter of rubber (mm)	Cross-sectional area of lead plug	Total thickness of rubber (mm)	Design axial stress (N/mm^2)
LRB	0.392	1500	Twice area of a standard type*	300	5

*:The diameter of lead plug is about 0.28 times that of rubber

3.2 Analytical modelling

An analytical model was made for an ABWR having an LRB base isolation system. The upper structure was modelled as a lumped mass using elastic beam elements. Damping of the strain energy proportional type and a damping coefficient of 0.03 were assumed. The isolation layer was modelled as a horizontal spring and two elastic rotational springs. The horizontal spring was modelled as multiple shear spring (MSS) which could take into account the interaction of bi-directional movement. The restoring force characteristics of the MSS for one axis direction was modelled as a modified bi-linear. The hardening phenomenon of the LRB was ignored in the analysis. Only hysteretic damping was assumed at the isolation layer. The analytical model is shown in Figure 1 and the natural vibration period of the analytical model is shown in Table 2.

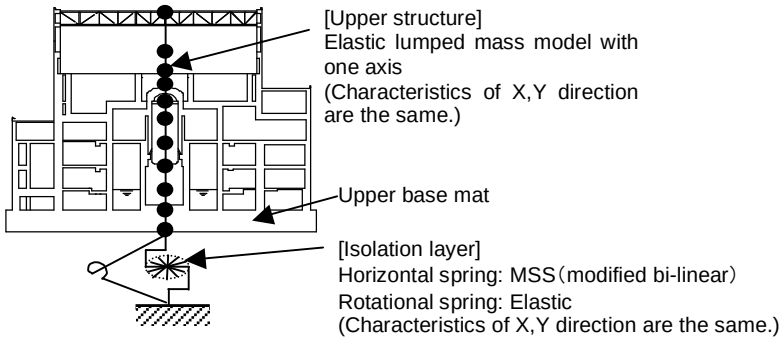

Figure 1. Analytical model

Table 2. Natural vibration period of the base-isolated reactor building

	Fixed upper base mat	Equivalent stiffness at =100% of LRB
First order natural period (s)	0.16	2.31

:shear strain of isolation layer

4 GROUND MOTION

Many types of ground acceleration motions made by different methods were used as input motions. The abbreviated designation of the ground motions are outlined in Table 3. The ground motions are classified into the following three types of waves based on how they were made.

a. "Artificial waves" with maximum acceleration of 1,040cm/s^2 and the same target spectrum

b. "Synthesized waves" made by the fault model, which simulates the motion caused by the fault

c. "Observed waves" amplified to the same level as the artificial waves

Table 3. Outline of ground motions and abbreviated designation

No.	Earthquake name		input direc-tion	abbreviated designation	max. acc. (cm/s^2)
(1)	Artificial waves (having the same target spectrum)	Standard wave（random phase）	X	RANDOM_S_STN	1,040
(2)		Phase wave having different random phase from (1) (PHS(RDM))	Y	RANDOM_S_PHS	
(3)		Phase wave with EW phase of (7)	X	SGF_S_EW_PHS	
(4)		Phase wave with NS phase of (8)	Y	SGF_S_NS_PHS	
(5)		Phase wave with EW phase of (9)	X	EGF_S_EW_PHS	
(6)		Phase wave with NS phase of (10)	Y	EGF_S_NS_PHS	
(7)	Synthesized waves	Synthesized wave combined hybrid method to stochastic Green's function	X	SGF_H_EW_FLT	996
(8)			Y	SGF_H_NS_FLT	733
(9)		Synthesized wave combined hybrid method to empirical Green's function	X	EGF_H_EW_FLT	814
(10)			Y	EGF_H_NS_FLT	881
(11)	Observed waves	EL Centro（1940.05.18）	X	ELCE EW	1,040
(12)			Y	ELCE NS	1,691
(13)		Taft（1952.07.21）	X	TAFT EW	1,040
(14)			Y	TAFT NS	903
(15)		HACHINOHE（1968.05.18）	X	HACHI EW	1,040
(16)			Y	HACHI NS	1,325

The Artificial waves were subdivided into a motion with random phase (Standard wave), a motion with different random phase (PHS (RDM)) and motions with synthesized wave phases (Phase wave). The Synthesized waves were subdivided into waves calculated by a hybrid method combined with the Stochastic Green's function using a fault model and those calculated by the hybrid method combined with the Empirical Green's function. NS and EW phases of the synthesized waves were given simultaneously as the motion was made. The El centro (1940.5.18), Taft (1952.7.21) and HACHINOHE (1968.5.18) recodes were selected as the Observed waves. These waves were amplified to the same level as the maximum acceleration of the artificial waves. We determined the amplification ratio according to the results of the preliminary response analysis by uni-directional input using each amplified motion having NS and EW components whose maximum acceleration was 1,040cm/s^2. We selected the amplification ratio of the component to reach the bigger maximum response displacement of these two components. The acceleration time history and the acceleration response spectrum of the artificial waves and the synthesized waves are shown in Figure 2 and Figure 3.

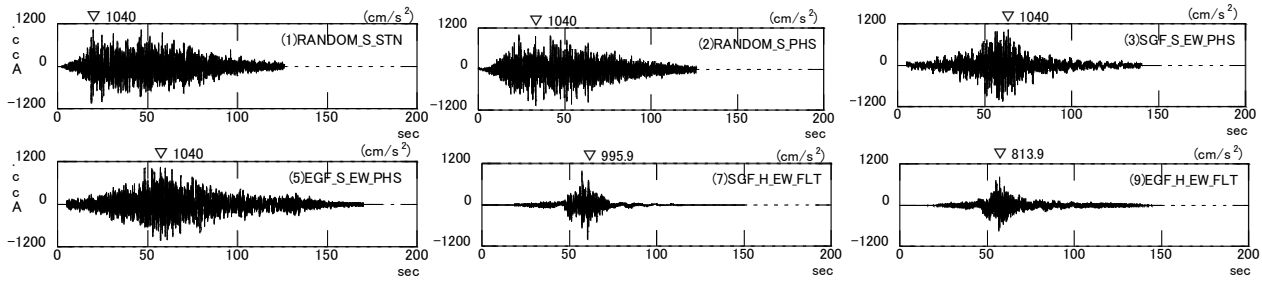

Figure 2. Time history of ground motions

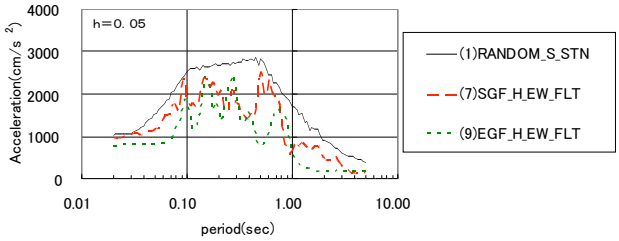

Figure 3. Response spectra of ground motions

5 INFLUENCE OF ORTHOGONAL GROUND MOTION

5.1 Input earthquake motions

Seismic response analyses were conducted parametrically for the base-isolated reactor building subjected to horizontal bi-directional earthquake motion using the many motions indicated in Section 4 to examine the influence of orthogonal ground motions. The response analyses were conducted for uni- (X direction) and bi-directional (X and Y direction) inputs. The maximum accelerations of the orthogonal ground motions were selected to be 0.5 and 0.75 times the original ground motion for the artificial waves.

5.2 Analysis results

The analysis results for bi-directional input were compared with those for uni-directional input. The maximum response acceleration and the maximum response displacement for (1) the Standard wave and (2) the PHS(RDM), and for the SGF_S_PHS wave ((3),(4)) are shown in Figure 4. The maximum response accelerations in the main direction (X direction) are slightly different for the uni- and bi-directional inputs caused by the influence of the orthogonal inputs (Y direction). For the displacement response, however, for the standard wave input there is a remarkable difference and the maximum response displacements increase with increase in orthogonal input level. Thus, the equivalent stiffness of the layer is decreased by the orthogonal input, and the natural vibration period of the isolation layer become longer. For the SGF_S_PHS input there is no remarkably increasing trend of response displacement with increasing orthogonal input, compared with the results for the standard wave input. The horizontal load – horizontal displacement interaction curve of the isolation layer for the uni-directional input (X direction) are compared with those for the bi-directional inputs when the orthogonal input level is 0.5 times the original in Figure 5. For the bi-directional inputs the hysteresis curve is more complicated than that for the uni-directional inputs and a partially negative inclination can be seen in the curve. The increasing rate of the maximum response displacement at the isolated layer for the bi-directional inputs compared to those for the uni-directional input is shown in Figure 6. In the synthesized wave inputs and the observed wave inputs we define the main axis by direction θ in which direction the response displacement at the isolation layer reaches a maximum value for the bi-directional inputs. The increasing rate for the bi-directional inputs compared to that for the uni-directional inputs using the uni-directional input motion projected in the main axis direction ($X' = X \cdot \cos\theta + Y \cdot \sin\theta$) is also shown in Figure 6. Figure 6 indicates that the maximum increasing rate is about 1.3 times for an artificial wave with random phase and about 1.1 times for the other input waves.

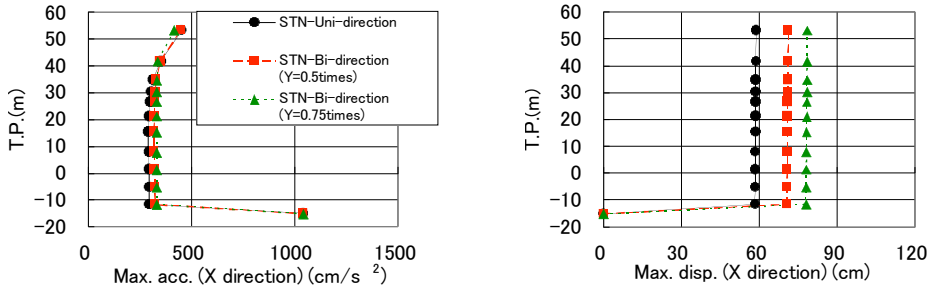

(a) RANDOM_S_STN (the orthogonal input: RANDOM_S_PHS) (Uni-: (1), Bi-: (1)+(2))

Figure 4. Results of analyses for bi-directional inputs using Artificial waves-1

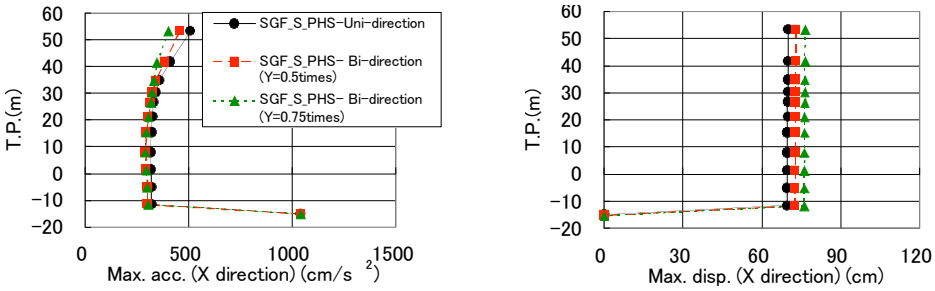

(b) SGF_S_PHS (Uni-:(3), Bi-:(3)+(4))

Figure 4. Results of analyses for bi-directional inputs using Artificial waves-2

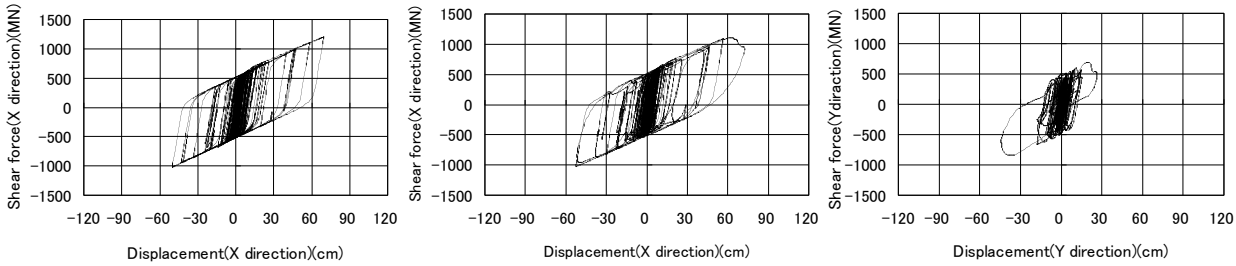

(a) Uni-directional input((3)) (b) Bi-directional input (Y= 0.5 times)((3)+(4))

Figure 5. Relationship between horizontal load and horizontal displacement for isolation layer (SGF_S_PHS)

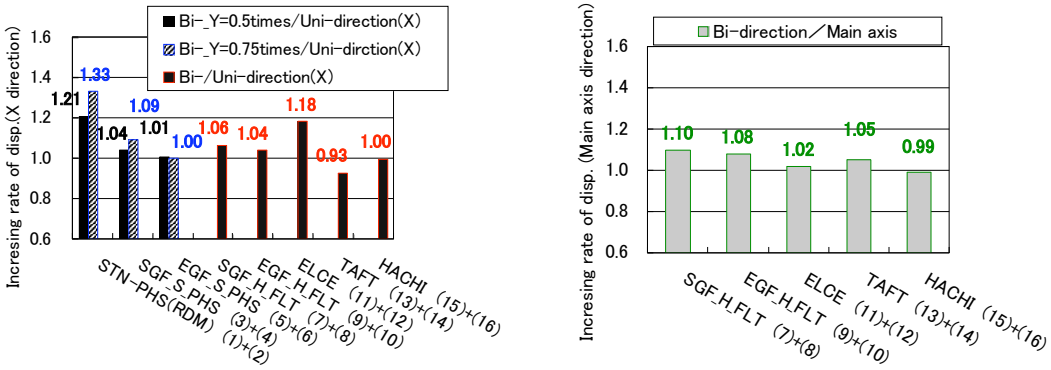

(a) Bi- (X direction)/ Uni-directional input (b) Bi- (Main axis direction)/Uni-directional input using the motions projected in the main axis direction

Figure 6. Increasing rate of displacement for isolation layer

6 INFLUENCE OF LEAD TEMPERATURE RISE

As one of the fluctuations of the characteristics of LRB, the yield load decreases with temperature rise of the lead plug caused by earthquake energy absorption. Earthquake response for uni-directional input was analyzed here considering this reduction of yield load for the horizontal spring of the isolation layer.

6.1 Analytical method considering temperature rise of lead plug

The method for response analysis taking into account the influence of temperature rise was in accordance with Part 1. In this method, the response analysis was conducted by varying the yield load through lead temperature while momentarily calculating the earthquake energy absorbed by the lead bearing on the assumption that the whole of the absorbed energy would be converted into higher lead temperature. At the same time, a heat transfer analysis was conducted in order to evaluate the heat radiation from the lead to the outside. The relationship between lead temperature and lead yield stress was based on the proposed formula

in Figure 7. The yield stress was set to become zero at the lead melting point of 327.5 deg. C as a function monotonically decreasing with temperature.

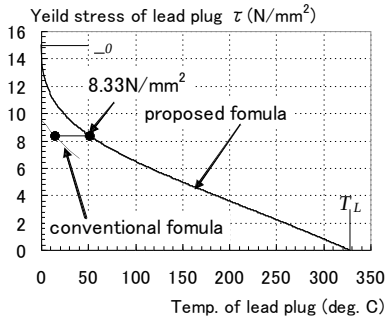

$\tau_o = 15.0(N/mm^2)$

$T_L = 327.5(℃)$

Figure 7. Relationship between temperature and yield stress of lead plug

The yield load of the LRB as the basis for the conventional formula of temperature dependence for design was based on the third cycle of repetitive load. In the third cycle, however, the temperature of the lead plugs had already increased due to energy absorption. This temperature was experimentally evaluated and the conventional formula of temperature dependence for design was shifted to a higher temperature side by approximately 35 deg. C to form the newly proposed formula. The earthquake response was analyzed for both cases, where the temperature rise was and was not considered. The initial temperature was set to 15 deg. C for the former case. The yield stress of lead in the latter case was assumed to be constant at the yield stress for design at 15 deg. C and thus to amount to 8.33 N/mm^2.

6.2 Input earthquake motions

Three types of artificial waves of earthquake motions were used: RANDOM_S_STN and SGF_S_EW_PHS having the same target spectrum, but with different phase characteristics, as well as SGF_H_EW_FLT of the earthquake motion based on a fault model. For SGF_S_EW_PHS, the effects of the difference in input level were examined by also inputting 0.8 and 1.2 times the reference input level of 1,040 cm/s^2.

6.3 Analysis results

Table 4 compares the maximum displacement of the isolation layer with and without lead temperature rise. Although the linear limit strain of the rubber bearing (displacement: 90 cm) was exceeded by a input 1.2 times for SGF_S_EW_PHS, the hardening phenomenon of the rubber bearing was ignored in the analysis.

Table 4. Maximum response displacement of isolation layer

Earthquake wave		Max. acc. of input motion (cm/s^2)	Max. response displacement of isolation layer (cm)	
			With considering lead tempereture rise	Without considering lead tempereture rise
Phase wave (SGF_S_EW_PHS)	0.8 times	832	51.6	50.3
	1.0 time	1,040	77.2	69.5
	1.2 times	1,248	109.1	93.0
Standard wave (RANDOM_S_STN)		1,040	63.2	58.3
Synthesized wave (SGF_H_EW_FLT)		996	27.3	28.3

Figure 8 compares the rate of displacement increase when the temperature rise was taken into account with the case where it was neglected. The rate becomes higher for a phase wave with increase in input level. This may be attributable to the fact that the amount of earthquake energy absorbed by the rubber bearing increases to raise the lead temperature, which in turn further reduces its yield stress. The displacement increased by approximately 10% for the phase wave and standard wave at the reference input level when taking the temperature rise into consideration. To the contrary, a slightly smaller displacement was shown in case of a synthesized wave when the temperature rise was taken into account. This is because, as is known from the relationship between lead temperature and yield stress, the yield stress is evaluated higher at temperatures below approx. 50 deg. C than when neglecting temperature rise and the lead temperature amounts to approximately 30 deg. C at maximum displacement.

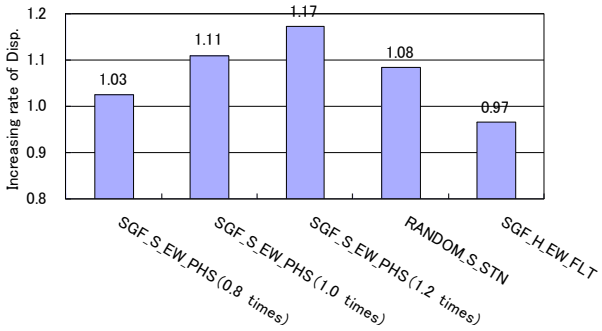

Figure 8. Increasing rate of displacement for isolation layer (considering / not considering temperature rise)

Figure 9 shows the maximum response accelerations and the maximum response horizontal displacements with and without considering temperature rise. The values for the phase wave are those at the reference input level. As for the response accelerations, the influence of temperature rise is small for the phase wave and standard wave, while it tends to vary in dependence for the synthesized wave. Figure 10 represents the relationship between load and deformation of the isolation layer. It can be seen that the yield load gradually decreases when the influence of temperature rise is taken into account. Figure 11 shows the time history of isolation layer displacement and lead temperature for the phase wave where the lead temperature rise is considered. The lead temperature has reached approx. 90 deg. C at maximum displacement. As can be seen from Figure 12, which compares the time history of yield stress of the lead plugs with the phase wave input level, the larger the input, the lower the lead yield stress.

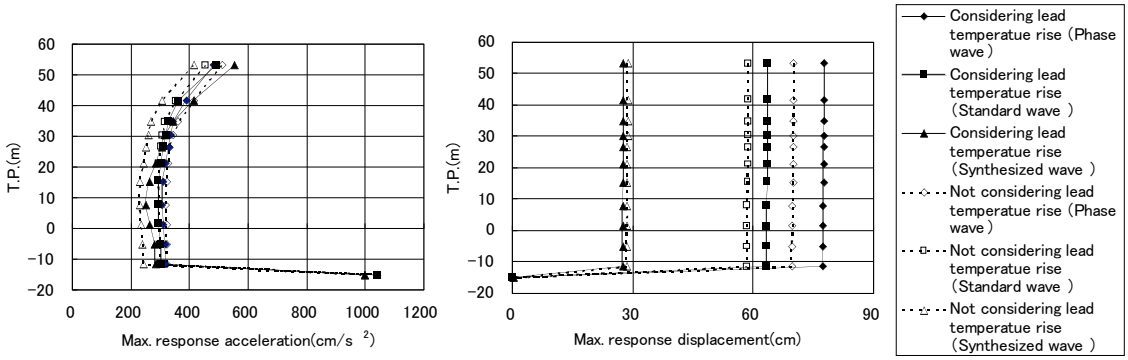

Figure 9. Maximum building response

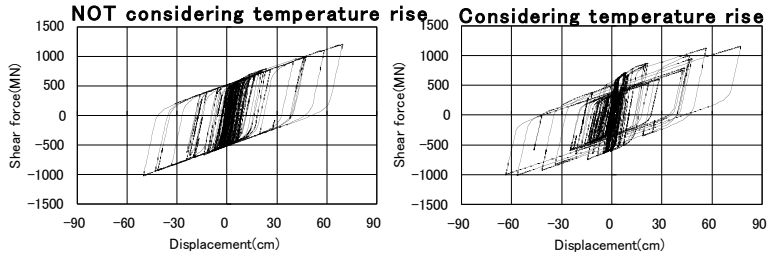

a. Phase wave (SGF_S_EW_PHS)

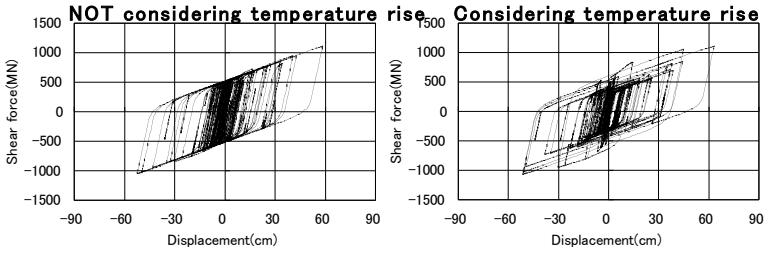

b. Standard wave (RANDOM_S_STN)

Figure 10. Relationship between shear force and displacement of isolation layer-1

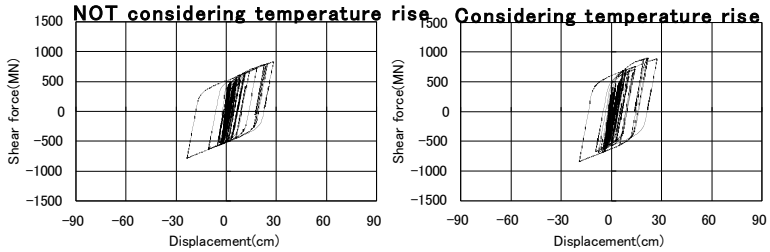

c. Synthesized wave (SGF_H_EW_FLT)

Figure 10. Relationship between shear force and displacement of isolation layer-2

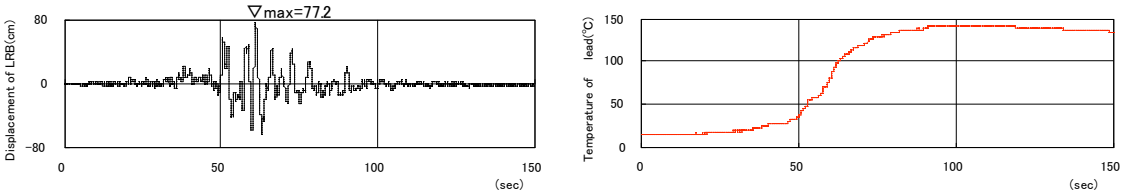

a. Displacement of isolation layer b. Temperature of lead

Figure 11. Time history of displacement of isolation layer and temperature of lead (at 1.0 times input)

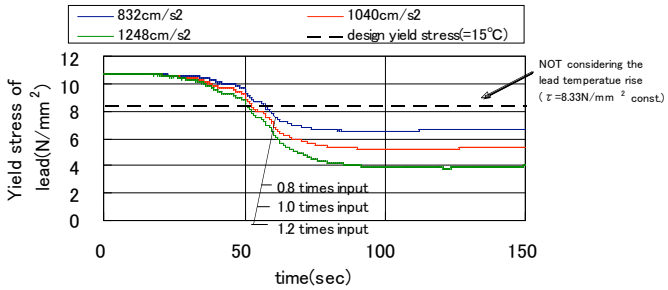

Figure 12. Time history of lead yield stress

7 INFLUENCE OF COMBINED FLUCTUATION FACTORS

As the principal fluctuation factors of the LRB characteristics affecting the maximum displacement response of a base-isolated reactor building using the LRB, the horizontal bi-directional earthquake motions (orthogonal input) were examined in Section 5 and the yield resistance reduction along with temperature rise of the lead plugs was discussed in Section 6. The influence of the combined factors including fluctuations of rubber bearing characteristics as discussed also for general base-isolated buildings was examined here.

7.1 Analytical model and input earthquake motions

The model shown in Section 3 was taken as the basis for the analytical model, while the analytical method stated in Section 6 was used when taking the temperature rise into consideration. The fluctuations of the LRB, which is considered for design of general base-isolated buildings were set by combining three factors, namely, product tolerance, aging and environmental temperature variation, so that the response displacement of the isolation layer may become largest, i.e., the secondary stiffness and the yield load of the LRB declined by 15% and 30% for the standard case respectively.

The input earthquake motions were set as a pair of SGF_S_EW_PHS and SGF_S_NS_PHS by selecting an artificial wave having the target spectrum of the earthquake motions, as stated in Section 4. Those waves have the phase of the synthesized wave as the phase characteristics. The EW phase wave was entered in the X direction, while the NS phase wave was entered in the Y direction. Incidentally, the input level in the Y direction was set to 0 (uni-directional input), 0.5 and 0.75 times that in the X direction.

7.2 Analysis results

Table 5 gives the maximum response displacement of the isolation layer. “The standard case” means that where the temperature rise and the fluctuations are not taken into account. “R direction” means the direction in which the largest amplitude as vector is indicated. In the standard case, the maximum response

displacement was within the linear strain limit (displacement: 90 cm) even by bi-directional input. If the fluctuations and the temperature rise were taken into account, it exceeded the linear strain limit by bi-directional input in case of (b)+(c) of Input2 and (b),(c),(b)+(c) of Input3. It exceeded the strain limit only slightly in case of Input2.

Table 5. Maximum response displacement of isolation layer

Input direc-tion	Max. response displacement(cm)									Max. response displacement(cm)		
	(a) Standard case			(b) Considering LRB's fluctuactions			(c) Considering lead temperature rise			(b)+(c)		
	X	Y	R	X	Y	R	X	Y	R	X	Y	R
Input1	69.5	-	69.5	75.7	-	75.7	77.2	-	77.2	83.5	-	83.5
Input2	72.4	44.3	77.4	76.4	46.3	80.9	81.3	48.8	85.6	94.8	46.8	97.4
Input3	76.0	66.0	84.9	76.8	66.9	90.1	89.4	72.3	95.3	103	91.5	128

Legends
Input1: Uni-directional input, (Max. acc. in the X direction: 1,040 cm/s^2)
Input2: Bi-directional input (Y=0.5 times) (Max. acc. in the X and Y direction: 1,040 and 520 cm/s^2)
Input3: Bi-directional input(Y=0.75 times) (Max. acc. in the X and Y direction: 1,040 and 780 cm/s^2)
X: X direction, Y: Y direction, R: R direction

Figure 13 shows the distribution of maximum response displacement and the maximum response acceleration in the X direction by unidirectional input in the standard case and bi-directional input with combined fluctuation factors where the input level in the Y direction was 0.5 times that in the X direction. Taking the fluctuation factors into consideration for the uni-directional input in the standard case was accompanied by increased displacement and a slightly lowered acceleration. Figure 14 indicates the relationship between horizontal load and horizontal displacement of the isolation layer in the X direction where the fluctuation factors are taken into account. The case where the input level in the Y direction was 0.5 times that in the X direction was set for the bi-directional input. Figure 15 shows the increasing rate of maximum displacement in the X direction for uni-directional input in the standard case. The maximum increasing rates for the cases where the input levels in the Y direction were 0.5 and 0.75 times those in the X direction were 1.36 and 1.48, respectively.

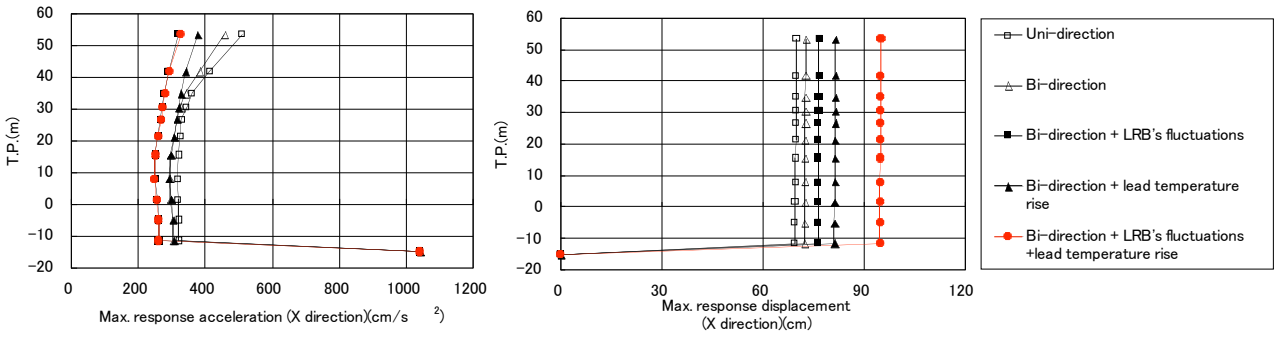

Figure 13. Maximum response in X direction taking into account combined fluctuations

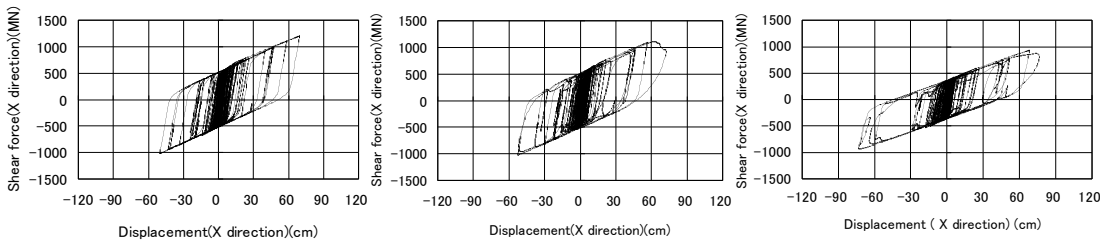

a. Uni-directional input (Standard case)

b. Bi-directional input (Standard case)

c. Bi-directional input +LRB's fluctuations

Figure 14. Relationship between horizontal load – horizontal displacement of isolation layer-1

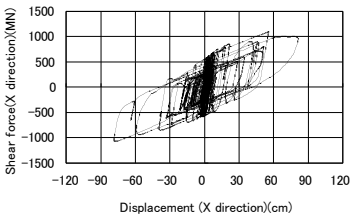

d. Bi-directional input
+Lead temperature rise

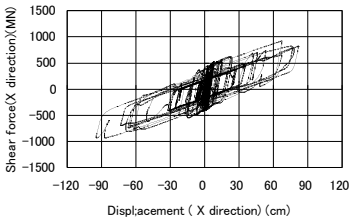

e. Bi-directional input
+LRB's fluctuations
+Lead temperature rise

Figure 14. Relationship between horizontal load – horizontal displacement of isolation layer-2

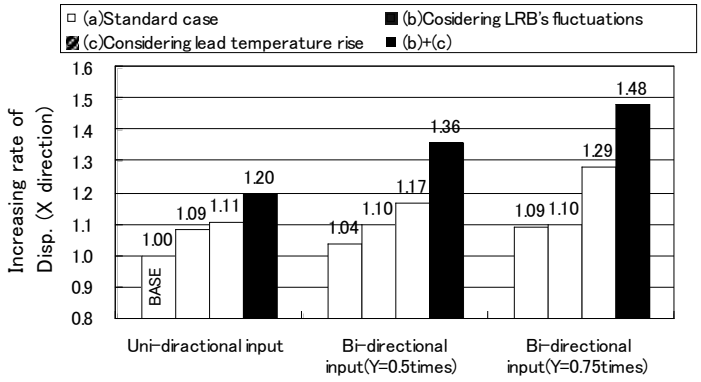

Figure 15. Increasing rate of displacement of isolation layer (X direction)

8 CONCLUSION

A base-isolated reactor building using an LRB was assumed to be located in a district of high seismic intensity to analytically examine the influence of the isolation system on building response through various fluctuation factors.

It was examined first by use of an artificial wave, a synthesized wave and an observed wave how an orthogonal seismic input affects the maximum response displacement. It was confirmed as a result that the influence varies with earthquake wave so that the largest rate of displacement increase of the isolation layer amounted to approx. 30% of that for a random phase within the scope of this study.

Next, an analysis taking into account the temperature rise of the lead plugs was performed for a uni-directional input. Consequently, the displacement of the isolation layer increased by approx. 10% due to the lead temperature rise caused by earthquake energy absorption. It was also ascertained that the influence varies in dependence on the input level and the characteristics of the earthquake motions.

It was also investigated how fluctuations of LRB characteristics affect the displacement response of the isolation layer. Lead yield stress lowered by the lead temperature rise and the influence by horizontal bi-directional earthquake motions (orthogonal input) including the fluctuations discussed for general base-isolated buildings were considered as fluctuation factors. Although the extent of the effects by these factors depend on the characteristics and input level of the earthquake motions, the displacement increment for the standard case which is not taking into account the fluctuation factors was at the most 1.5 even if the all fluctuation factors were taken into account.

In future study on base-isolated structures in districts of high seismic intensity, it seems necessary to further examine on the various fluctuation factors, earthquake motions to be adopted and input levels to be considered in orthogonal directions.

REFERENCE

Architectural Institute of Japan. Recommendation for the Design of Base Isolated Buildings (in Japanese) 2001. 406 p. ISBN4-8189-0529-1